

Neural Power-Optimal Magnetorquer Solution for Multi-Agent Formation and Attitude Control

Yuta Takahashi¹

Abstract—This paper presents an efficient algorithm for finding the power-optimal currents of magnetorquer, a satellite attitude actuator in Earth orbit, for multi-agent formation and attitude control. Specifically, this study demonstrates that a set of power-optimal solutions can be derived through sequential convex programming and proposes a method to approximate these solutions using a deep neural network (DNN). The practicality of this DNN model is demonstrated through numerical simulations of formation and attitude control.

Index Terms—Distributed Space System, Multi-agent Control, Non-Convex Programming.

I. INTRODUCTION

THE magnetic field provides a sophisticated control system along with navigation that is applied in medicine, biomimetic robotics, and aerospace fields. Typically, they are generated by coils wounding conductive wires around magnetic materials or an air core; passing current through these conductors generates a magnetic field. Its interaction with the surrounding magnetic ones provides their relative position and orientation while generating electromagnetic forces and torques. The aerospace community has originally utilized them in Earth orbit as efficient actuators for satellite attitude control [4]. They have referred to the coils as magnetorquer (MTQ) and recently utilized MTQ in micro-gravity for satellite docking [10], and inter-satellite state estimation [18].

The multi-agent control methodologies using MTQ have mainly been developed in aerospace fields as one of the low-thrust actuators. Previous work drives MTQ with the direct current (DC) and alternating current (AC) methods. The AC method provides higher functionality than DC one: no average interaction with the Earth’s direct magnetic field and different frequency magnetic fields. Moreover, the AC method realizes 6-DoF control [8], [11], [12], i.e., they can output arbitrary control force and torque for an arbitrary number of agents. In the DC method, two agents can output arbitrary electromagnetic force and torque [8]. Still, in the formation control for a larger number of agents, the electromagnetic torque cannot be controlled and acts as a disturbance to the system. Therefore, in previous studies, the evaluation function $\|\tau\|$ is optimized. MTQ formation control solves conventional actuator problems and provides a promising direction, particularly for proximity operation over extended periods.

However, MTQ control requires the frequent computation of MTQ current solutions for high-precision control. The MTQ control system must convert command control to current signals, with coordinated allocation among satellites, which traditionally incurs high computational costs. This process is a nonconvex constraint. Thus, power-optimal optimization is a nonconvex optimization problem and belongs to the Quadratically Constrained Quadratic Program (QCQP), which are NP-hard to solve in general. Thus,

To this end, we provide an efficient algorithm to find and approximate the power-optimal magnetorquer solution by machine learning technique. First, we show that a set of power-optimal solutions can be derived through convex relaxation via the standard (Shor) semidefinite program (SDP) relaxation. Then, we propose a technique to approximate them using a DNN. We demonstrate the practicality of this DNN model: autonomous formation and attitude control numerical simulations.

II. PRELIMINARIES

This section summarizes MTQ control methodologies and learning-based techniques for functional approximation.

A. Magnetorquer Control Under Nonholonomic Constraints

This subsection introduces the dipole approximation of magnetic interaction and the modulation technique of the AC method for 6-DoF (six degrees of freedom) control. Assuming first that all n agents have the circular triaxial MTQ and j th magnetic moment $\mu_j(t)$ [Am²] at time t is

$$\mu_j(t) = N_t c(t) A \left(1 + \frac{(\mu_r - 1)}{(1 - N_d + \mu_r N_d)} \right) \mathbf{n} \in \mathbb{R}^3$$

where N_t is the number of coil turns; $c(t)$ is the current strength; A is the area enclosed by the coil; \mathbf{n} is the unit vector perpendicular to the plane of the coil; l is the length of the coil; $N_d = 4(\ln(l/r) - 1)/((l/r)^2 - 4\ln(l/r))$ [2]. A “Far-field” model [13] provides the approximated magnetic field $B_k(\mu_k, r_{jk})$ [T], which is accurate if the relative distance exceeds twice the diameter of the coil [5]:

$$B_k(\mu_k, r_{jk}) = \frac{\mu_0}{4\pi d_{jk}^3} (3M_k \mathbf{e}_r - \mu_k) \quad (1)$$

where $M_k = \mu_k \cdot \mathbf{e}_r$, $d_{jk} = \|\mathbf{r}_{jk}\|$, and $\mathbf{e}_r = \mathbf{r}_{jk}/d_{jk}$. The computationally expensive exact model could be used for closer distance, which is called the Near-filed model [10], [13]. The Far-filed model derive electromagnetic force

¹Graduate Student, Department of Mechanical Engineering, Tokyo Institute of Technology, Ookayama Meguro, Tokyo 152-8552, Japan takahashi.y.c1@m.titech.ac.jp

$\mathbf{f}_{j \leftarrow k}(\boldsymbol{\mu}_{j,k}, \mathbf{r}_{jk}) = \nabla(\boldsymbol{\mu}_j \cdot B_k)$ and electromagnetic torque exerted on the j -th agent by the k -th one:

$$\mathbf{f}_{j \leftarrow k} = \frac{3\mu_0}{4\pi d^4} ((\boldsymbol{\mu}_k \cdot \boldsymbol{\mu}_j - 5M_k M_j) \mathbf{e}_r + M_k \boldsymbol{\mu}_j + M_j \boldsymbol{\mu}_k).$$

$$\boldsymbol{\tau}_{j \leftarrow k}(\boldsymbol{\mu}_{j,k}, \mathbf{r}_{jk}) = \boldsymbol{\mu}_j \times B_k$$

Let us assume that j th agent's MTQ for $j \in [1, n]$ are driven sinusoidal with angular frequency ω_{f_j} [rad/s], i.e., the AC method. Here, we assume that a th and b th dipole are

$$\boldsymbol{\mu}_a(t) = \boldsymbol{\mu}_{\text{ampa}} \sin(\omega_{fa}t + \theta), \quad \boldsymbol{\mu}_b(t) = \boldsymbol{\mu}_{\text{ampb}} \sin(\omega_{fb}t)$$

where amplitudes $\boldsymbol{\mu}_{\text{amp}j} \in \mathbb{R}^3$, the j th angular frequency ω_{f_j} [rad/s], and the phase differences $\theta \in \mathbb{R}^3$ between a th and b th dipole moments. Then, the time-varying electromagnetic force $\mathbf{f}(\boldsymbol{\mu}_a(t), \boldsymbol{\mu}_b(t), \mathbf{r}_{ba})$ and torque $\boldsymbol{\tau}(\boldsymbol{\mu}_a(t), \boldsymbol{\mu}_b(t), \mathbf{r}_{ba})$ are written down as

$$\begin{cases} \mathbf{f}(\boldsymbol{\mu}_a(t), \boldsymbol{\mu}_b(t), \mathbf{r}_{ba}) = (\kappa_1 + \kappa_2) \mathbf{f}(\boldsymbol{\mu}_{\text{ampa}}, \boldsymbol{\mu}_{\text{ampb}}, \mathbf{r}_{ba}) \\ \boldsymbol{\tau}(\boldsymbol{\mu}_a(t), \boldsymbol{\mu}_b(t), \mathbf{r}_{ba}) = (\kappa_1 + \kappa_2) \boldsymbol{\tau}(\boldsymbol{\mu}_{\text{ampa}}, \boldsymbol{\mu}_{\text{ampb}}, \mathbf{r}_{ba}) \\ \kappa_1, \kappa_2 = \pm \frac{1}{2} \cos((\omega_{fa} \mp \omega_{fb})t + \theta) \end{cases}$$

AC-method assume $\boldsymbol{\mu}_{\text{amp}j}$ and θ are constant during specific one cycle T that derived on Eq. (3) later. Then, their time-varying vectors $\mathbf{f}, \boldsymbol{\tau}$ take 0 for $\omega_a \neq \omega_b$ in first-order averaged dynamics [8], i.e., the agent that uses ω_{f_j} does not interact with those of $\omega_{f_k} \neq \omega_{f_j}$.

B. Kinematics Control for 6-DoF Magnetorquer Control

We mention the simultaneous control strategy of the electromagnetic force and torque with 3-axis RW using "Kinematics" for n -agent system [8]. We consider the n satellite with 3-axis MTQ and assume that $m \in [1, n]$ satellites (from a total of n) are equipped with 3-axis RWs. MTQ control can not control all absolute positions and attitudes of multi-agents from the viewpoint of a holonomic and nonholonomic system, i.e., entire linear and angular momentum remains unchanged: Let us $r_c = \sum_j m_j r_j / \sum_j m_j$

$$\sum_{j=1}^n \left(m_j \mathbf{r}_j \times \frac{d\mathbf{r}_j}{dt} + \mathbf{I}_j \cdot \boldsymbol{\omega}_j \right) + \sum_{j=1}^m \mathbf{h}_j = \mathbf{L}$$

$$\Leftrightarrow A_{(n,m)} \zeta = \begin{bmatrix} m_1 [r_1^i]_{\times}, \dots, m_n [r_n^i]_{\times}, \\ C^{I/B_1} J_1, \dots, C^{I/B_n} J_n, \\ C^{I/B_1}, \dots, C^{I/B_m} \end{bmatrix} \begin{bmatrix} \dot{r}^i \\ \omega^b \\ \xi^b \end{bmatrix} = 0$$

where $A_{(n,m)} \in \mathbb{R}^{3 \times (6n+3m)}$, the states $\zeta \in \mathbb{R}^{6n+3m}$ and $\xi^b \in \mathbb{R}^{3m}$, and $\xi_j^{b_j} = h_j^{b_j} - \frac{1}{m} L^{b_j}$. Then, let $S_{(n,m)} \in \mathbb{R}^{(6n+3m) \times (6n+3m-3)}$ be the tangent space of angular momentum conservation, i.e., $S_{(n,m)} \in \text{Null Space}(A_{(n,m)})$, which are smooth, linearly independent vector fields, and the controller based on this fields could be generated by MTQ.

C. Deep Neural Network Approximation

Deep Neural Network (DNN) represents the functional mapping from given inputs x into some outputs $f(x, \theta)$ such as a $(L+1)$ -layer neural network:

$$f(x, \theta) = W^{L+1} \phi(W^L (\dots \phi(W^1 x + b^1) \dots) + b^L) + b^{L+1}$$

where the activation function $\phi(\cdot)$ and the DNN parameters θ include the DNN weights $\theta_w = W^1, \dots, W^{L+1}$ and the DNN bias $\theta_b = b^1, \dots, b^{L+1}$.

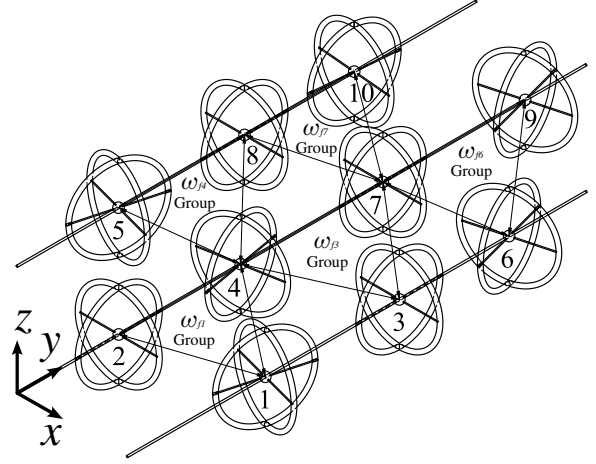


Fig. 1: Example of the multi-leader guidance concept (Ten magnetorquer are divided into five groups with five AC frequencies: $\omega_{f1,3,4,6,7}$).

III. MULTI-LEADER-BASED SIMULTANEOUS CONTROL OF RELATIVE POSITION AND ABSOLUTE ATTITUDE

We introduce multi-leader-based dipole allocation to decentralize multi-agent into small groups and focus on one leader satellite group in the following subsections. This increases the system's scalability and reduces computational loads. First, we formulate the directed multi-leader graph with multi-followers. Consider the N satellites nodes $\mathcal{V} = \{1, \dots, N\}$ and let us assign specific agents into leaders subset $\mathcal{V}_l \in \mathcal{V}$. For the edge set $\mathcal{E} \subseteq \mathcal{V} \times \mathcal{V}$, the edge $(j, k) \in \mathcal{E}$ denotes that k -th node can obtain some information such as their relative distance or interactions from j -th and they are called neighbors whose sets are $\mathcal{N}_j = \{k \mid (j, k) \in \mathcal{E}\}$. For the directed multi-leader graph $\mathcal{G}^{\text{ml}}(\mathcal{V}, \mathcal{E}^{\text{ml}})$, edge $(j, k) \in \mathcal{E}^{\text{ml}}$ describes the hierarchical relationships of $k \in \mathcal{V}_l$ and $j \in \mathcal{V}/k$, i.e., j -th satellite is following k -th one. We label leader satellite \mathcal{V}_l with their follower satellites as "l Group":

$$\mathfrak{g}_l = \{l, f \in \mathcal{V} \mid (f, l) \in \mathcal{E}_l^{\text{ml}}\}$$

$$\mathcal{E}^{\text{ml}} = \mathcal{E}_1^{\text{ml}} \cap \dots \cap \mathcal{E}_N^{\text{ml}}$$

Note that if j th satellite does not have followers, $\mathfrak{g}_l = j$ and $\mathcal{E}_N^{\text{ml}} = \{j\}$.

For given $\mathcal{G}^{\text{ml}}(\mathcal{V}, \mathcal{E}^{\text{ml}})$, let us assume that different unique frequencies ω_{c_i} [rad/s] are assigned in each satellite \mathcal{V} . Then, the selected follower satellites drive the coil with the leader's AC frequency. and use AC frequency ω_{f_j} . This extends dipole moment in Eq. (5) into the multi-frequency dipole moment as Assuming that j th satellite's magnetorquers drive an alternating magnetic field with angular frequency ω_{f_j} [rad/s] for $j = 1, \dots, n$. Then, its magnetic moment $\boldsymbol{\mu}_j(t)$ is approximated by a time-varying vector as

$$\boldsymbol{\mu}_j(t) = \sum_{l \in \mathcal{V}_l} \sum_{(j,k) \in \mathcal{E}_l} (s_{j \leftarrow k} \sin(\omega_{f_1} t) + c_{j \leftarrow k} \cos(\omega_{f_1} t)) \quad (2)$$

where sine wave amplitude $s_j \in \mathbb{R}^3$, cosine wave amplitude $c_j \in \mathbb{R}^3$. where k is the number of AC frequency groups the j th satellite belongs to. The total $2\omega_f$ disturbance of electromagnetic force and torque exerted on the j -th satellite

by the entire system is $f, \tau_{j(2\omega_f)} = \sum_{k=1}^n f, \tau_{2\omega_f}(t)$. The main point is that we show the frequency modulation work. The values of ω_{f_i} [rad/s] of each satellite should be carefully selected for the first-order approximation and attitude noises attenuation. Its least common multiple is defined as

$$\text{s.t. : } \begin{cases} \mathbf{f}_{j(\text{avg})} \equiv \int_T \sum_{k \neq j} \mathbf{f}_{j \leftarrow k}(\boldsymbol{\mu}_k(\tau), \boldsymbol{\mu}_j(\tau), \mathbf{r}_{jk}) \frac{d\tau}{T}, \\ \boldsymbol{\tau}_{j(\text{avg})} \equiv \int_T \sum_{k \neq j} \boldsymbol{\tau}_{j \leftarrow k}(\boldsymbol{\mu}_k(\tau), \boldsymbol{\mu}_j(\tau), \mathbf{r}_{jk}) \frac{d\tau}{T}. \end{cases}$$

One cycle T is derived to cancel out the coupling between different frequencies [8]

$$T = \frac{1}{k_{\text{int}}} \text{lcm} \left(\frac{2\pi k_{\text{int}}}{2\omega_{f_i}}, \frac{2\pi k_{\text{int}}}{|\omega_{f_i} - \omega_{f_j}|}, \frac{2\pi k_{\text{int}}}{\omega_{f_i} + \omega_{f_j}} \right) \quad (3)$$

where $\text{lcm}(\cdot)$ is the least common multiple, $k_{\text{int}} \in \mathbb{R}$ is coefficient to make elements of $\text{lcm}(\cdot)$ integer, and i, j is arbitrary index that satisfies $1 \leq i < j \leq n$. Note that the necessary conditions to hold $T \leq T_{\text{max}}$ for given T_{max} are

$$\omega_{f_i} \geq \frac{\pi}{T_{\text{max}}}, |\omega_{f_i} - \omega_{f_j}| \geq \frac{2\pi}{T_{\text{max}}}, \omega_{f_i} + \omega_{f_j} \geq \frac{2\pi}{T_{\text{max}}}$$

such that elements of $\text{lcm}(\cdot)$ satisfies $T \leq T_{\text{max}}$. One easy way to select ω_{f_i} is choosing as $\omega_{f_i} = i \times \frac{2\pi}{T_{\text{max}}}$ such that $T = \frac{T_{\text{max}}}{k_{\text{int}}} \text{lcm}(\frac{k_{\text{int}}}{2i}, \frac{k_{\text{int}}}{|i-j|}, \frac{k_{\text{int}}}{i+j}) = T_{\text{max}}$. It is worth noting that the current should be updated based on the maximum frequency $(2n+1) \times \frac{2\pi}{T_{\text{max}}}$ for this approximation to hold. Its frequency ω_{f_i} on Eq. (5) is set to be about 50-100 rad/s in this study.

IV. POWER-OPTIMAL DIPOLE ALLOCATION BY CONVEX-OPTIMIZATIONS

This subsection presents global power-optimal dipole calculation by multiple convex programmings for the power-efficient control of n agents. We prove the uniqueness of this global minimum, and the results are used to construct DNNs of optimal dipole allocation in the next section. Let $\mathbf{f}_{c_j}, \boldsymbol{\tau}_{c_j}$ for $j \in [1, n]$ be defined as the given command 6-DoF control by the arbitrary controller. We must convert these command values into the associated dipole solutions or current to realize them by magnetic interaction. Specifically, the optimal dipole solutions satisfies the following power optimal problem:

$$\min : \frac{1}{2} \|\mathbf{m}\|^2 \quad \text{s.t. : } \begin{cases} \mathbf{f}_{c_j} = \mathbf{f}_{j(\text{avg})}, \\ \boldsymbol{\tau}_{c_j} = \boldsymbol{\tau}_{j(\text{avg})}, \end{cases} \quad \text{for } j \in [1, n], \quad (4)$$

which is QCQP with $6n$ equality constraints, where $T = \text{lcm}(2\pi/\omega_{f_{a_j}})$. Conventionally, with each increase in the number of agents and the dimension of the problem, finding the global optimal solution becomes computationally expensive.

A. Minimal Representation of Dipole Solution

Let us consider the time-varying dipole $\boldsymbol{\mu}_j(t)$ on Eq. (5) with $\mu_{\text{DC}j} = 0$ for simplicity. We could rewrite $\boldsymbol{\mu}_j(t)$ by using the vectors $\mathbf{s}_j, \mathbf{c}_j \in \mathbb{R}^3$, without the loss of generality,

$$\begin{aligned} \boldsymbol{\mu}_j(t) &= \boldsymbol{\mu}_{\text{amp}j} \sin(\omega_{f_j} t + \boldsymbol{\theta}_j) \\ &= \mathbf{s}_j \sin(\omega_{f_j} t) + \mathbf{c}_j \cos(\omega_{f_j} t) \end{aligned} \quad (5)$$

where

$$\begin{aligned} \boldsymbol{\mu}_{\text{amp}j(i)} &\equiv \sqrt{\mathbf{s}_{j(i)}^2 + \mathbf{c}_{j(i)}^2}, \\ \mathbf{s}_{j(i)} &= \boldsymbol{\mu}_{\text{amp}j(i)} \cos(N_c \pi + \theta_0 + \boldsymbol{\theta}_{j(i)}) \\ \mathbf{c}_{j(i)} &= \boldsymbol{\mu}_{\text{amp}j(i)} \sin(N_s \pi + \theta_0 + \boldsymbol{\theta}_{j(i)}) \end{aligned} \quad (6)$$

where $\boldsymbol{\theta}_j \in \mathbb{R}^3$ are phases for j th MTQ with its trigonometric relationship. Since sin and cos waves do not interact on average, the first-order averaged input $\mathbf{f}_{j \leftarrow k(\text{avg})}, \boldsymbol{\tau}_{j \leftarrow k(\text{avg})} \in \mathbb{R}^3$ exerted on j th dipole by k th one is

$$\begin{aligned} \mathbf{f}_{j \leftarrow k(\text{avg})} &= \{f(s_j, s_k, r_{jk}) + f(c_j, c_k, r_{jk})\}/2 \\ \boldsymbol{\tau}_{j \leftarrow k(\text{avg})} &= \{\boldsymbol{\tau}(s_j, s_k, r_{jk}) + \boldsymbol{\tau}(c_j, c_k, r_{jk})\}/2 \end{aligned} \quad (7)$$

such as $\mathbf{f}_{j \leftarrow k}(t) = \mathbf{f}_{j \leftarrow k(\text{avg})} + \mathbf{f}_{2\omega_f}(t)$ where $2\omega_f$ disturbance $\mathbf{f}_{2\omega_f}(t)$ [8], which is unique to the AC-based magnetorquers control. Based on this principle, we derive the first-order time-averaged model for controller design without the trigonometric functions. Then, we define the overall dipole vector:

$$\mathbf{m}_N(t) = \mathbf{m}_N(\boldsymbol{\mu}_{\text{amp}}, \boldsymbol{\theta}, t) = [\mathbf{s}_N; \mathbf{c}_N] \in \mathbb{R}^{6n}.$$

where $\mathbf{s}_N = [\mathbf{s}_1; \dots; \mathbf{s}_n] \in \mathbb{R}^{3n}$, $\mathbf{c}_N = [\mathbf{c}_1; \dots; \mathbf{c}_n] \in \mathbb{R}^{3n}$. Since we rely on the first-order averaged model as mentioned in subsection II-A, these formulations $\boldsymbol{\mu}_j(t)$ are redundant; $\mathbf{m}_N(\boldsymbol{\mu}_{\text{amp}}, \boldsymbol{\theta} + \theta_0, t)$ with arbitrary $\theta_0 \in \mathbb{R}$ could achieve the same evaluation function results on Eq. (4). To erase these redundant, we newly introduce the symmetric matrix variable \mathfrak{X} :

$$\mathbf{s}_N \mathbf{s}_N^\top + \mathbf{c}_N \mathbf{c}_N^\top = [\mathbf{s}_N \quad \mathbf{c}_N] [\mathbf{s}_N \quad \mathbf{c}_N]^\top \equiv \mathfrak{X} \in \mathbb{S}^{3n \times 3n}.$$

where $\text{rank}(\mathfrak{X}) \leq 2$ and this formulation does not include θ_0 such that

$$\mathfrak{X}_{(3(j-1)+l, 3(k-1)+m)} = \boldsymbol{\mu}_{\text{amp}j(l)} \boldsymbol{\mu}_{\text{amp}k(m)} \cos(\boldsymbol{\theta}_{j(l)} - \boldsymbol{\theta}_{k(m)})$$

for $j, k \in [1, n]$ and $l, m \in [1, 3]$. Note that this transformation extends $6n$ dimensional vector \mathbf{m}_N into $3n(3n+1)/2$ one, but could be expressed later.

$$\mathfrak{X} = \int_T \boldsymbol{\mu}_N \boldsymbol{\mu}_N^\top \frac{d\tau}{T}, \quad \begin{cases} \boldsymbol{\mu}_{\text{amp}N} = \sqrt{\text{Diag}(\mathfrak{X})} \\ \text{Cos}\mathfrak{D}\boldsymbol{\theta} = \mathfrak{X} \oslash (\boldsymbol{\mu}_{\text{amp}N} \boldsymbol{\mu}_{\text{amp}N}^\top) \end{cases}$$

where $\boldsymbol{\mu}_{\text{amp}N} \equiv [\boldsymbol{\mu}_{\text{amp}1}; \dots; \boldsymbol{\mu}_{\text{amp}n}] \in \mathbb{R}^{3n}$ that satisfies $\boldsymbol{\mu}_{\text{amp}n} \geq 0$ and $\text{Cos}\mathfrak{D}\boldsymbol{\theta} \in \mathbb{R}^{3n \times 3n}$, and where \oslash means the element-wise division, i.e., Hadamard division, and

$$\text{Cos}\mathfrak{D}\boldsymbol{\theta}_{(3(j-1)+l, 3(k-1)+m)} = \cos(|\boldsymbol{\theta}_{j(l)} - \boldsymbol{\theta}_{k(m)}|)$$

B. Reduced Dimensional First-Order Time-Averaged Model

We first simplify the far-filed magnetic filed-based electromagnetic force and torque model and reduce the decision parameters by using line-of-sight frame $\mathcal{L}\mathcal{O}\mathcal{S}_{j/k}$ fixed in k -th agent to see j -th agent. We define the coordinate whose x -axis is aligned with v and y -axis is orthogonal to v and w where $v, w \in \mathbb{R}^3$ are given the arbitrary vectors. Its coordinate transformation matrix is

$$\mathcal{C}(^a v, ^a w) = [\mathbf{e}_x = \text{nor}(^a v), \mathbf{e}_y, \mathbf{e}_x \times \mathbf{e}_y] \in \mathbb{R}^{3 \times 3} \quad (8)$$

where $e_y = \text{nor}(S^{(a)v}a_w)$. Based on Eq. (8), we define its coordinate transformation matrix $C^{O/LOS_{jk}} \in \mathbb{R}^{3 \times 3}$ as

$$C^{O/LOS_{jk}} = C^{(o)r_{jk}, S^{(o)f_j} r_{jk}}. \quad (9)$$

Note that x -axis in \mathcal{LOS} is aligned with r_{jk} and a given the desired force f_{jk} in frame \mathcal{O} remains $x-y$ plane in frame \mathcal{LOS} , i.e., ${}^{LOS}r_{jk} = [{}^a r_{jk}; 0; 0]$ and ${}^{LOS}f_{jk}(3) = 0$. This simplifies the first-order time-averaged model on Eq. (7) as bilinear polynomial formulation:

$$u_{L \leftarrow F}^{los} = \frac{1}{2} \frac{\mu_0}{4\pi} Q_{d_{LF}} (s_F^{los} \otimes s_L^{los} + c_F^{los} \otimes c_L^{los}) \in \mathbb{R}^6 \quad (10)$$

where $u_{L \leftarrow F}^{los} = [f_{L \leftarrow F}^{los}; \tau_{L \leftarrow F}^{los}]$, the norm of the relative distance $d_{jk} = \|r_{jk}\|$ and the matrix $Q_{d_{jk}} \in \mathbb{R}^{6 \times 9}$ are

$$Q_{d_{jk}} = \frac{1}{d_{jk}^4} \left[\begin{array}{c} [-6, 0_3, 3, 0_3, 3] \\ 0, 3, 0, 3, 0_5 \\ 0_2, 3, 0_3, 3, 0_2 \end{array} \right]; d_{jk} \left[\begin{array}{c} 0_5, 1, 0, -1, 0 \\ 0_2, 2, 0_3, 1, 0_2 \\ 0, -2, 0, -1, 0_5 \end{array} \right]$$

As a result, the 9-dimensional decision parameters, u and position $r \in \mathbb{R}^3$, on Eq. (7) are reduced into a 6-dimensional one $\chi_s = [d; f_{F \leftarrow L(1,2)}^{los}; \tau_{F \leftarrow L}^{los}] \in \mathbb{R}^6$. Their solutions could be infinite numbers [8], and one easy way for two agents to do this is to predetermine constants $[s_{F0}^{los}; c_{F0}^{los}]$ to yield $[s_L^{los}; c_L^{los}]$ uniquely by the nature of the bilinear polynomial:

$$\begin{bmatrix} s_L^{los} \\ c_L^{los} \end{bmatrix} = \left\{ \frac{\mu_0}{8\pi} Q_d ([s_{F0}^{los}, c_{F0}^{los}] \otimes E_3) \right\}^{-1} u_{L \leftarrow F}^{los}. \quad (11)$$

This leads to a decentralized strategy, but their dipole moment lacks optimality, which is crucial for limited resources. This motivates us to derive the optimal power consumption solutions even for the case $N = 2$ in the next subsection.

Remark 1. We briefly note how to give $[s_{F0}^{los}, c_{F0}^{los}]$ on Eq. (11). Without the loss of generality, we could set $\theta_{j(1)}^{los} = 0$ among θ_j^{los} as

$$s_{F0} = \begin{bmatrix} \mu_{\text{amp}F(1)} \\ \mu_{\text{amp}F(2)} \cos \theta_{F(2)} \\ \mu_{\text{amp}F(3)} \cos \theta_{F(3)} \end{bmatrix}, c_{F0} = \begin{bmatrix} 0 \\ \mu_{\text{amp}F(2)} \sin \theta_{F(2)} \\ \mu_{\text{amp}F(3)} \sin \theta_{F(3)} \end{bmatrix}$$

where the subscripts $\{los\}$ are dropped in the remainder. Then, a simple calculation verifies the following $[s_{F0}^{los}, c_{F0}^{los}]$ guarantees the existence of inverse:

$$\mu_{\text{amp}F(1)} \mu_{\text{amp}F(2)} \mu_{\text{amp}F(3)} \sin(\theta_{F(2)} - \theta_{F(3)}) \neq 0.$$

The perpendicular vector $\mu_{F\perp}$ of $\mu_F(t)$ based on Eq. (5) is Its orthogonal vector $\mu_{F0\perp} \in \mathbb{R}^3$ satisfies

$$\mu_{F0\perp} // (c_{F0} \times s_{F0}) = \begin{bmatrix} \mu_{\text{amp}j(2)} \mu_{\text{amp}j(3)} \sin(\theta_{j(2)} - \theta_{j(3)}) \\ \mu_{\text{amp}j(3)} \mu_{\text{amp}j(1)} \sin(\theta_{j(3)} - \theta_{j(1)}) \\ \mu_{\text{amp}j(1)} \mu_{\text{amp}j(2)} \sin(\theta_{j(1)} - \theta_{j(2)}) \end{bmatrix}$$

Then, the dipoles with components only in $l \in [1, 3]$ -th axis, i.e., $\mu_{F\perp} = \delta_{il} \in \mathbb{R}^3$ is achieved by $\mu_{\text{amp}F(l)} = 0$ that do not satisfies the above conditions where δ_{il} is Kronecker delta. We show that the lack of an arbitrary component in LOS falls into the singularity of the inverse matrix.

We generalize the first-order time-averaged model on Eq. (10) into the case $N \geq 2$. We derive the sine and cosine wave amplitude s_j, c_j in user-defined arbitrary frame $\{\mathcal{A}\}$

for given the positions vectors $r_j^a \in \mathbb{R}^3$ and a command input $u^a = [u_1^a; \dots; u_N^a] \in \mathbb{R}^{6N}$. Let us define line-of-sight frame $\{\mathcal{LOS}_{j/k}\}$ fixed in k -th agent to see j -th agent, and its coordinate transformation matrix $C^{A/LOS_{j/k}}$ are defined by Eq. (8):

$$C^{A/LOS_{j/k}} = C(r_{jk}^a, S(f_j^a) r_{jk}^a). \quad (12)$$

Then, Eq. (10) derives the constraints for the dipole solutions:

$$\frac{8\pi}{\mu_0} u_j^a = \sum_{k \neq j} Q_{d_{jk}}^a (s_k^a \otimes s_j^a + c_k^a \otimes c_j^a), j \in [1, N] \quad (13)$$

where $Q_{d_{jk}}^a \in \mathbb{R}^{6 \times 9}$ are

$$Q_{d_{jk}}^a = (I_2 \otimes C^{A/LOS_{jk}}) Q_{d_{jk}} (C^{LOS_{jk}/A} \otimes C^{LOS_{jk}/A}).$$

Let us define the matrix $Q_{d_{jk}}^i \in \mathbb{R}^{3 \times 3}$ that satisfies $\text{vec}(Q_{d_{jk}}^i) = Q_{d_{jk}(i,:)}^{a\top}$, and this converts the i th component on Eq. (13) for $i \in [1, 6]$ into

$$\begin{aligned} \frac{8\pi}{\mu_0} u_{j(i)}^a &= \sum_{k \neq j} Q_{d_{jk}(i,:)}^a (s_k^a \otimes s_j^a + c_k^a \otimes c_j^a) \\ &= \text{tr} [s_j^a \sum_{k \neq j} (s_k^{a\top} Q_{d_{jk}}^{i\top}) + c_j^a \sum_{k \neq j} (c_k^{a\top} Q_{d_{jk}}^{i\top})] \\ &= \text{tr} [(s_j^a s_j^{a\top} + c_j^a c_j^{a\top}) \hat{Q}_j^i] \end{aligned} \quad (14)$$

where we apply Roth's column lemma [21] for the second equality, \hat{Q}_j^i means subvector such that, for arbitrary vector $x \in \mathbb{R}^{3n}$: $\hat{x}_j = [x_{(1:3j-3)}; x_{(3j+1:3n)}] \in \mathbb{R}^{3n-3}$, and the matrix $\hat{Q}_j^i \in \mathbb{R}^{3 \times 3n-3}$ is

$$\hat{Q}_j^i = [\hat{Q}_{d_{j1}}^i \quad \dots \quad \hat{Q}_{d_{j(j-1)}}^i, \quad \hat{Q}_{d_{j(j+1)}}^i \quad \dots \quad \hat{Q}_{d_{jN}}^i].$$

C. Power-Optimal Dipole Allocation for N agents Group Including One Leader Agent

Then, the optimization problem for power-optimal dipole solution for N agents are

$$\begin{aligned} \min : J_p(m_N) &= \frac{1}{2} \|m_N\|^2 = \frac{1}{2} (s_N^\top W s_N + c_N^\top W c_N) \\ \text{s.t.} : \frac{8\pi}{\mu_0} u_{j(i)}^a &= \text{tr} [(s_j^a s_j^{a\top} + c_j^a c_j^{a\top}) \hat{Q}_j^i] \end{aligned} \quad (15)$$

where $i \in [1, 6]$, $j \in [1, N-1]$.

1) Case $N = 2$: *Strict Global Power-Optimal Dipole Allocation*: Next, let us consider to derive the dipole solution $m_{LF} = [s_L; s_F; c_L; c_F] \in \mathbb{R}^{12}$ for two agents on Eq. (10) to achieve a given reduced χ_s by the controller. and formulate a non-convex optimization problem:

$$\begin{aligned} \min : J_p(m_{LF}) &= \frac{1}{2} \|m_{LF}\|^2 \\ \text{s.t.} : h(m_{LF}) &= Q_d (s_F \otimes s_L + c_F \otimes c_L) - \frac{8\pi}{\mu_0} u_{L \leftarrow F}^{los} = 0 \end{aligned} \quad (16)$$

which belongs to the QCQP with six equality constraints. Note that $u_{L \leftarrow F}^{los}$ on the following problems are divided by the constant related $\mu_0 = 4\pi e^{-7}$ Tm/A to avoid excessive trials and errors on calculations. Then, we define the Lagrangian $L_2(m_{LF}, \lambda_{N=2}) = J_p(m_{LF}) + \lambda^\top h(m_{LF})$ and Lagrange multiplier vector $\lambda_{N=2} \in \mathbb{R}^6$. The Lagrange dual problem

associated with the primal problem on Eq. (16), which is convex and efficiently solvable, is

$$\max : J_d = \frac{-\lambda^\top u_{L \leftarrow F}^{los}}{\mu_0 / (8\pi)} \quad \text{s.t.} : P_\lambda = \begin{bmatrix} E_3 & R_\lambda \\ R_\lambda^\top & E_3 \end{bmatrix} \succeq 0 \quad (17)$$

where $R_\lambda \in \mathbb{R}^{3 \times 3}$ satisfies $\text{vec}(R_\lambda) = Q_d^\top \lambda$. Despite QCQP including Eq. (7) is not convex, strong duality holds, i.e., no optimal duality gap exists, for QCQP with one quadratic inequality constraint provided Slater's condition holds [22]. The following presents the global optimal power consumption solutions for two agents to realize command control.

Theorem IV.1. *Consider the relative position r_{LF} and the command input $u_{L \leftarrow F}^{los} = [f_{L \leftarrow F}^{los}; \tau_{L \leftarrow F}^{los}] \in \mathbb{R}^6$ from b -th agent to a -th one. Let $\lambda^* \in \mathbb{R}^6$ be defined as the optimal Lagrange multiplier vector $\lambda^* \in \mathbb{R}^6$ of the Lagrange dual problem on Eq. (17). Then, a global-optimum solution of the non-convex optimization on Eq. (16) is $[s_F^*, c_F^*] = -R_{\lambda^*}^\top [s_L^*, c_L^*]$ and $[s_L^*, c_L^*]$ satisfies*

$$s_L^* = \mu_{\text{amp}L} \cos \theta_L, \quad c_L^* = \mu_{\text{amp}L} \sin \theta_L$$

$$\mu_{\text{amp}L} = \begin{bmatrix} \sqrt{\mathcal{L}_1} \\ \sqrt{\mathcal{L}_2} \\ \sqrt{\mathcal{L}_3} \end{bmatrix}, \quad \begin{cases} |\theta_{L(1)} - \theta_{L(2)}| = \cos^{-1}(\mathcal{L}_4 / \sqrt{\mathcal{L}_1 \mathcal{L}_2}) \\ |\theta_{L(3)} - \theta_{L(1)}| = \cos^{-1}(\mathcal{L}_5 / \sqrt{\mathcal{L}_3 \mathcal{L}_1}) \\ |\theta_{L(2)} - \theta_{L(3)}| = \cos^{-1}(\mathcal{L}_6 / \sqrt{\mathcal{L}_2 \mathcal{L}_3}) \end{cases}$$

where \mathcal{L}_j is derived by $\text{vec}(Q_d^i) = Q_d(i, :)^T$ and

$$-\text{tr} \left[R_{\lambda^*} Q_d^{i\top} \begin{bmatrix} \mathcal{L}_1 & \mathcal{L}_4 & \mathcal{L}_5 \\ * & \mathcal{L}_2 & \mathcal{L}_6 \\ * & * & \mathcal{L}_3 \end{bmatrix} \right] = \frac{8\pi}{\mu_0} u_{L \leftarrow F}^{los}(i), \quad i \in [1, 6] \quad (18)$$

Proof. First, we will show that the non-convex primal problem on Eq. (16) and associated Lagrange dual problem on Eq. (17) hold strong duality, i.e., $J_p(m^*) = J_d(\lambda^*)$. Consider the

$$U = \text{vec}(Q_d(i, :))$$

Since optimal points of any optimization problem that strong duality holds satisfy the KKT conditions [22], we add these into an original problem on Eq. (16). The Roth's column lemma [21] convert $\lambda^\top Q(s_F \otimes s_L + c_F \otimes c_L)$ into $\text{tr}[R_\lambda^\top (s_L s_F^\top + c_L c_F^\top)]$ where $R_\lambda \in \mathbb{R}^3$ satisfies $\text{vec}(R_\lambda) = Q^\top \lambda$. This simplifies $L(m, \lambda)$ as

$$L(m, \lambda) = \frac{1}{2} m^\top (I_2 \otimes P_\lambda) m - \frac{8\pi}{\mu_0} \lambda^\top u_{L \leftarrow F}^{los}.$$

where $u_{L \leftarrow F}^{los} = [f_{L \leftarrow F}^{los}; \tau_{L \leftarrow F}^{los}]$. Then, the first-order necessary conditions for optimal solutions are $\frac{\partial L}{\partial \lambda} = g(m) = 0$, $\frac{\partial L}{\partial m} = 0$ and the second equality constraints is added into Eq. (17). Here, $\frac{\partial L}{\partial m} = (I_2 \otimes P_\lambda) m = 0$ yields

$$P_\lambda \begin{bmatrix} s_L \\ s_F \end{bmatrix} = P_\lambda \begin{bmatrix} c_L \\ c_F \end{bmatrix} = 0 \Rightarrow \begin{cases} [s_L, c_L] + R_\lambda [s_F, c_F] = 0 \\ [s_F, c_F] + R_\lambda^\top [s_L, c_L] = 0, \end{cases}$$

This relationship also yields

$$\begin{cases} [s_L, c_L] = R_\lambda R_\lambda^\top [s_L, c_L] \\ [s_F, c_F] = R_\lambda^\top R_\lambda [s_F, c_F] \end{cases} \Rightarrow \begin{cases} \|s_L\| = \|R_\lambda s_F\| = \|s_F\| \\ \|c_L\| = \|R_\lambda c_F\| = \|c_F\| \end{cases}$$

Therefore, global-optimum solutions m^* satisfies

$$f(m^*) = \|s_F^*\|^2 + \|c_F^*\|^2 = \|s_L^*\|^2 + \|c_L^*\|^2 = \text{const}$$

To fill these constraints, let us consider the variable transformation. Then, the use of the variable a_i yields the following equality for an arbitrary vector $x \in \mathbb{R}^9$ and associated matrix $X \in \mathbb{R}^{3 \times 3}$ such that $\text{vec}(X) = x$:

$$x^\top (s_F \otimes s_L + c_F \otimes c_L) = \text{tr}[X^\top (s_L s_F^\top + c_L c_F^\top)] \\ = -\text{tr}[R_\lambda X^\top (s_L s_L^\top + c_L c_L^\top)]$$

where we apply the Roth's column lemma and $(I_2 \otimes P_\lambda) m = 0$. For the above relationship, we substitute the following equation with the introduced variable \mathcal{L}_i such that

$$s_L s_L^\top + c_L c_L^\top \equiv \begin{bmatrix} \mathcal{L}_1 & \mathcal{L}_4 & \mathcal{L}_5 \\ * & \mathcal{L}_2 & \mathcal{L}_6 \\ * & * & \mathcal{L}_3 \end{bmatrix},$$

which reduces the degree of the entire polynomial on Eq. (10) and convexity the primal problem on Eq. (16). Replacing x on above relationship by $Q_d^\top(i, :) \in \mathbb{R}^9$ for $i \in [1, 6]$ reduces the constraints on Eq. (16) into linear equality Eq. (18). \square

2) *Case $N \geq 2$:* Next, we generalize two agents' results into N agents' ones to obtain power-optimal dipole solutions. The optimization problem for power-optimal dipole solution for N agents is Eq. (15) and the associated Lagrangian $L_N \in \mathbb{R}$ with the Lagrange multiplier vector $\hat{\lambda}_N \in \mathbb{R}^{6(N-1)}$ is

$$L_N(m_N, \hat{\lambda}_N) = \frac{1}{2} m_N^\top (I_2 \otimes P_{\hat{\lambda}_N}) m_N - \frac{\hat{\lambda}_N^\top \hat{u}^a}{\mu_0 / (8\pi)}$$

where use the reduced command $\hat{u}^a = [u_1^a; \dots; u_{N-1}^a] \in \mathbb{R}^{6(n-1)}$ and non-symmetric matrix $O_{\hat{\lambda}_N} \in \mathbb{R}^{3n \times 3n}$:

$$P_{\hat{\lambda}_N} = I_{3n} + O_{\hat{\lambda}_N} + O_{\hat{\lambda}_N}^\top, \quad \text{vec}(\hat{R}_{\lambda_j}^{jk}) = Q_d^{a\top} \lambda_j$$

$$O_{\hat{\lambda}_N} = \begin{bmatrix} O_3 & \hat{R}_{\lambda_1}^{12} & \dots & \hat{R}_{\lambda_1}^{1(N-1)} & \hat{R}_{\lambda_1}^{1N} \\ \hat{R}_{\lambda_2}^{21} & O_3 & \dots & \hat{R}_{\lambda_2}^{2(N-1)} & \hat{R}_{\lambda_2}^{2N} \\ \vdots & \vdots & \ddots & \vdots & \vdots \\ \hat{R}_{\lambda_{N-1}}^{(N-1)1} & \hat{R}_{\lambda_{N-1}}^{(N-1)2} & \dots & O_3 & \hat{R}_{\lambda_{N-1}}^{(N-1)N} \\ O_3 & O_3 & \dots & O_3 & O_3 \end{bmatrix}.$$

It is easy to see that $P_{\hat{\lambda}_N}$ is a positive definite matrix, otherwise there exist m_N such that $L_N(m_N, \hat{\lambda}_N) \rightarrow -\infty$. Finally, we derive optimal m_N^* on Eq. (15).

Theorem IV.2. *For N agents, consider their position vectors from arbitrary point $r_j \in \mathbb{R}^3$ for $j \in [1, n]$ and their command input $u^a \in \mathbb{R}^{6N}$. Let $\hat{\lambda}_N^* \in \mathbb{R}^{6(n-1)}$ be defined as the optimum solution of the Lagrange dual problem of Eq. (15):*

$$\text{OPT}_{\text{DUAL}} \max : J_{dN} = \frac{-\hat{\lambda}_N^{\top} \hat{u}^a}{\mu_0 / (8\pi)} \quad \text{s.t.} : P_{\hat{\lambda}_N^*} \succeq 0 \quad (19)$$

and this defines optimal $P_{\hat{\lambda}_N^*}$. Then, a global-optimum solution $m_N^* = [s_N^*; c_N^*] \in \mathbb{R}^{6N}$ of the non-convex optimization on Eq. (15) satisfies $s_N^* s_N^{\top} + c_N^* c_N^{\top} \equiv \mathfrak{X}$ and it derives

Algorithm 1 Convex Optimization-based Power-Optimal Dipole Allocation for 6-DoF MTQ Control of N -Agents

- 1: **Inputs:** position/command $r_j \in \mathbb{R}^3, \mathbf{u}_j \in \mathbb{R}^6, j \in [1, n]$
 - 2: **Outputs:** $\boldsymbol{\mu}_{\text{amp}N}^*, \boldsymbol{\theta}_N^* \in \mathbb{R}^{3n}$ and $\mu_j^a(t) \in \mathbb{R}^3, j \in [1, n]$
 - 3: Define the base frame $\{\mathcal{A}\}$ and derive r_j^a and u_j^a
 - 4: Solve $P_{\lambda_N^*} = \text{OPT}_{\text{DUAL}}\{r_j^a, u_j^a\}$ on Eq. (19)
 - 5: Solve $\mathfrak{X}_j^* = \text{OPT}_{\text{ODA}}\{r_j^a, u_j^a, P_{\lambda_N^*}\}$ on Eq. (20)
 - 6: Solve $\boldsymbol{\mu}_{\text{amp}N}^*, \boldsymbol{\theta}_N^* = \mathcal{EQ}_{\mu}\{\mathfrak{X}_j^*\}$
 - 7: Choose $\theta_0 \in \mathbb{R}$, e.g., $\theta_0^* = \arg \min \|\mu(t_-) - \mu(t_+, \theta_0)\|$
 - 8: Derive $\mu_j^a(t) = \boldsymbol{\mu}_{\text{amp}j}^* \sin(\omega_f t + \boldsymbol{\theta}_j^* + \theta_0)$
-

unique $\boldsymbol{\mu}_{\text{amp}}$ and $\boldsymbol{\theta}$ for $\mathbf{m}_N(t) = \mathbf{m}_N(\boldsymbol{\mu}_{\text{amp}}, \boldsymbol{\theta}, t)$ where the symmetric matrix $\mathfrak{X} \in \mathbb{R}^{3(n-1) \times 3(n-1)}$ satisfies

$$\frac{8\pi}{\mu_0} u_{j[i]}^a = \text{tr} \left[\mathfrak{X}_{[3j-2:3j, [1:3j-3, 3j+1:3n]]} \hat{\mathcal{Q}}_j^{i\top} \right], P_{\lambda_N^*} \mathfrak{X} = 0$$

where $i \in [1, 6], j \in [1, N-1]$.

Proof.

$$(I_2 \otimes P_{\lambda_N^*}) \mathbf{m}_N = 0 \Rightarrow P_j[s_j^a, c_j^a] + \hat{P}_j[\hat{s}_j^a, \hat{c}_j^a] = 0$$

□

For gained symmetric matrices $\mathfrak{X} \in \mathbb{R}^{3n \times 3n}$, we could convert them into optimal dipole solutions $\mathbf{m}_N^* \in \mathbb{R}^{6N}$.

Remark 2.

$$\begin{aligned} \text{OPT}_{\text{ODA}} : \mathfrak{X}^* &= \arg \min_{\mathfrak{X} \in \mathbb{S}^{3n \times 3n}, X_k \in \mathbb{P}^{3n \times 3n}} \text{trace}(\mathfrak{X}) + w_k e_k \\ \text{s.t. : } &\begin{cases} \left| \frac{8\pi}{\mu_0} u_{j[i]}^a - \text{tr} \left[\mathfrak{X}_{[3j-2:3j, [1:3j-3, 3j+1:3n]]} \hat{\mathcal{Q}}_j^{i\top} \right] \right| \leq \varepsilon_0 \\ e_k I_{n-r} - V_{k-1}^T X_k V_{k-1} \succeq \mathbf{0} \\ e_k \leq e_{k-1}, \end{cases} \end{aligned} \quad (20)$$

V. NEURAL POWER-OPTIMAL DIPOLE ALLOCATION

Finally, this subsection presents the methodology to construct the learning-based optimal dipole solutions by DNN that enable a power-efficient online dipole allocation. This study mainly uses an element-wise Rectified Linear Unit (ReLU) function $\phi(x) = \text{ReLU}(x)$ as an activation one. Note that its simpler operations $\text{ReLU}(x) = \max(0, x)$ is less computationally expensive than tanh and sigmoid. To cope with the curse of dimensionality for DNN, we choose the line-of-sight frame $\{L\} \equiv \{\mathcal{LOS}_{l/c}\}$ from center mass position $r_c \in \mathbb{R}^3$ into l th agent as the base frame:

$$r_c = \frac{\sum_{k \in \mathfrak{g}_l} m_k r_k}{\sum_{k \in \mathfrak{g}_l} m_k} \Rightarrow C^{O/L} = C(r_{1c}^o, S(f_j^o) r_{1c}^o).$$

Here, the use of $\{L\}$ reduces 3 dimension from their $9(N-1)$ dimensional input data.

$$\boldsymbol{\mu}_{\text{amp}j}, \boldsymbol{\theta}_j = \mathcal{M}_{\text{NODA}}(\hat{r}^l, \hat{f}^l, \hat{r}^l, \boldsymbol{\theta})$$

where o^l means the components in frame $\{L\}$ and the DNN parameters $\boldsymbol{\theta}$. Note that the proposed ‘‘NODA’’ models are agent-structure and control-system invariant if the far-field

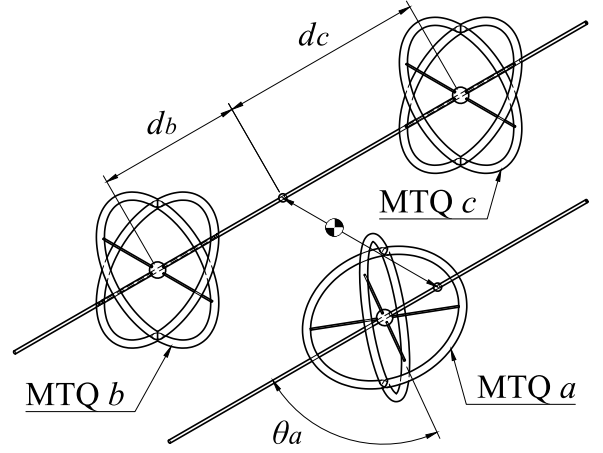


Fig. 2: This is the caption for one fig.

model is valid, i.e., the relative distance does not exceed twice the diameter of the coil as described in subsection II-A. The input data is normalized to the range $[0, 1]$, which is sufficient as it ensures evenly spaced values, making it suitable for learning. On the other hand, the output labels depend on the fourth power of position, and normalizing them can result in a significant variation in magnitude, including minimal values. To address this and improve the stability of the learning process, a logarithmic transformation is applied to compress the scale of the output labels.

Remark 3. Switching the values of $m(t_-)$ into $m(t_+)$ at time t could induce an impulse input. The large fluctuations may excite disturbances in the high-frequency band or cause chattering. To alleviate this, the free parameter θ could be chosen as $\theta^* = \arg \min \|\mu(t_-) - \mu(t_+, \theta)\|$. In the next subsection, we construct continuous gains using neural techniques to alleviate the additional chattering by discontinuously switching.

VI. SIMULATION VALIDATION

We validate our NODA algorithm and multi-leader strategy through the formation and attitude control experiments.

A. Formation Controller Design and Two Grouping Methods

We set our control goal; the desired positions are a regular triangle of r_d [m], and the desired angle of MTQ a $\theta_{ad} \in \mathbb{R}$ is 0. We define the base frame: the y axis is along with the linear track, and the z axis is perpendicular to the table. The origin is set such that the y axis penetrates the geometric center of MTQs b & c , and the x axis completes a right-handed orthogonal frame. Then, the positions of MTQs a & b & c , $p_{a,b,c} \in \mathbb{R}^3$ are defined and set to achieve our control goals as

$$p_{b,c} = [0; y_{b,c}(t); 0], p_a = \left[\frac{\sqrt{3}}{2} r_d; \frac{L_{\text{air}}}{2}; 0 \right]$$

where $y_b(t) < y_c(t)$.

$$y_{1d,2d} = (L_{\text{air}} \mp r_d)/2, \theta_{3d} = \xi_{1d}^{b_1} = \xi_{2d}^{b_2} = 0 \quad (21)$$

and their differential values $\dot{y}_{1d,2d}$ and $\dot{\theta}_{3d}$ are set to 0.

To compensate for the non-rotatability of the MTQs 1&2, we assume that the MTQs 1&2 have virtual 3-axis RWs and completely cancel out the torques generated in them. Since the excessive bias between the angular momentum of virtual RWs is avoided, these virtual RWs introduce the virtual states $\xi_j^{bj} = (h_j^{bj} - L^{bj}/m)$ in subsection II-B. The linear momentum conservation justifies the immobility of MTQ 3, but the air tracks' constraints should be compensated by aligning their force to parallel to the linear air track. Based on the above assumptions, we partially justify the mechanical constraints of linear track and air bearing for a 6-DoF control experiment.

We summarize the controllers to achieve the control goals of the relative position, absolute attitude, and a "virtual reaction wheel (RW)." For three MTQs to realize the arbitrary control command, we consider the two dipole allocation methods: the centralized dipole allocation NODA and the decentralized one on Eq. (11).

$$Z_{\text{cent}} = \begin{bmatrix} 0 & 0 & 0 \\ 0 & 0 & 0 \\ 1 & 1 & 0 \end{bmatrix}, \quad A_n = \begin{bmatrix} 0 & 1 & 1 \\ 1 & 0 & 1 \\ 1 & 1 & 0 \end{bmatrix}$$

$$Z_{\text{decent}} = \begin{bmatrix} 0 & 1 & 0 \\ 0 & 0 & 1 \\ 1 & 0 & 0 \end{bmatrix}, \quad A_1 = \begin{bmatrix} 0 & 1 & 0 \\ 1 & 0 & 0 \\ 0 & 0 & 0 \end{bmatrix},$$

$$A_2 = \begin{bmatrix} 0 & 0 & 0 \\ 0 & 0 & 1 \\ 0 & 1 & 0 \end{bmatrix}, \quad A_3 = \begin{bmatrix} 0 & 0 & 1 \\ 0 & 0 & 0 \\ 1 & 0 & 0 \end{bmatrix}.$$

Theorem VI.1. Let $x \in \mathbb{R}^{6n}$ be defined the states as $x = [p; \sigma]$ where position vectors $p \in \mathbb{R}^{3n}$ and arbitrary attitude parameters $\sigma \in \mathbb{R}^{3n}$. Consider

$$\begin{bmatrix} \dot{f}_c^i(L_l) \\ \dot{\hat{\tau}}_c^i(L_l) \end{bmatrix} = -(L_l \otimes I_6) \{K_p(x - x_d) + K_d(\dot{x} - \dot{x}_d)\} \in \mathbb{R}^{6n}$$

$$\dot{h}_{cl}^{bi} = -k_\xi \xi_l^{bi} = -k_\xi (h_l^{bi} - L_g^{bi}/m) \in \mathbb{R}^3, \text{ for } l \in [1, m-1]$$

where $L_n \in \mathbb{R}^{3 \times 3}$ is arbitrary laplacian matrix. Then, the auxiliary commands $u_x = [f_c^i; \hat{\tau}_c^i; \dot{h}_{c1}^{bi}] \in \mathbb{R}^{15}$ satisfies $u_x(L_n) = \sum_l u_x(L_l)$ where $L_n = \sum_l L_l$ and the control commands $u_c = [f_c^i; \tau_c^b; \dot{h}_c^b] \in \mathbb{R}^{21}$

$$u_c = B_{(3,2)}^{-1} M_{(3,2)} S_{(3,2)} u_x, \quad S_{(3,2)} = \begin{bmatrix} E_{(21)} \\ -C^{B_2/I} A_{(3,2)[:,1:21]} \end{bmatrix}$$

where the inertia and input matrix $M_{(n,m)} = \text{Diag}([M_p, M_\alpha, E_{3m}])$, $B_{(n,m)} \in \mathbb{R}^{(6n+3m) \times (6n+3m)}$:

$$B_{(n,m)}, B_{(n,m)}^{-1} = \begin{bmatrix} E_{3n} & 0 \\ E_{3n} & \mp E_{3n \times 3m} \\ 0 & E_{3m} \end{bmatrix}$$

achieve the control goal Eq. (21) as $t \rightarrow \infty$.

Proof. See the appendix of [8]. \square

B. Three Dipole Allocations and Neural Model Construction

Note that this comparison is along with sample optimal magnetometer solutions. Note that the non-rotatability of the MTQs in our experiment reduces attitude σ in Theorem VI.1 and $\hat{\tau}_c^b$ into θ_3 and $\hat{\tau}_c^b = -[0_8; 2k_{\theta p}(\theta_3 - \theta_{3d}) + 2k_{\theta d}(\dot{\theta}_3 -$

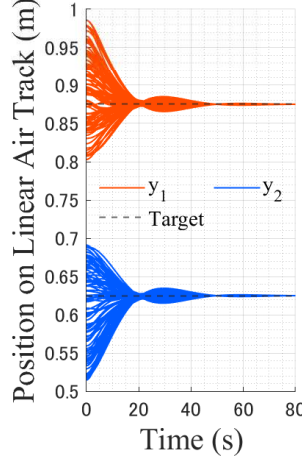


Fig. 3: (a) position

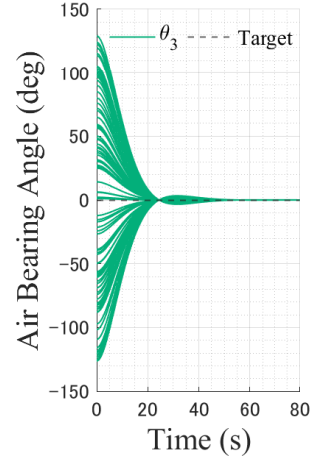


Fig. 4: (b) attitude

Fig. 5: Simulation results for sampling the optimal dipole allocations

Algorithm 2 Inverse Matrix-based Dipole Allocation for 6-DoF MTQ Control of 2-Agents based on Eq. (11)

- 1: **Inputs:** trial number n_{rand} , position/command $r_j \in \mathbb{R}^3$, $u_j \in \mathbb{R}^6$, $j \in [1, n]$
- 2: **Outputs:** $\mu_{\text{amp}N}^*$, $\theta_N^* \in \mathbb{R}^{3n}$ and $\mu_j^a(t) \in \mathbb{R}^3$, $j \in [1, n]$
 $\mu_L\{i\} = [s_L^{\text{los}}; c_L^{\text{los}}] \in \mathbb{R}^6$ and $\mu_F\{i\} = [s_{F0}^{\text{los}}; c_{F0}^{\text{los}}] \in \mathbb{R}^6$
- 3: Calculate $u_{L \leftarrow F}^{\text{los}}$, Q_d
- 4: **for** $i \in [1, n_{\text{rand}}]$ **do**
- 5: Generate a normalized random vectors $k_1, k_2 \in \mathbb{R}^3$
- 6: Calculate $[j_1; j_2] = \left\{ \frac{\mu_0}{8\pi} Q_d ([k_1, k_2] \otimes E_3) \right\}^{-1} u_{L \leftarrow F}^{\text{los}}$
- 7: $J_{\{i\}} = \sqrt{\|j_{1,2}\|}$
- 8: $\mu_L\{i\} = \frac{1}{\sqrt{\|j_{1,2}\|}} [j_1, j_2]$, and $\mu_F\{i\} = \sqrt{\|j_{1,2}\|} [k_1, k_2]$
- 9: **end for**
- 10: Choose $\mu_{L,F}^* = \mu_{L,F\{i\}}$ such that $i^* = \arg \min J_{\{i\}}$

$\theta_{3d}) \in \mathbb{R}^9$. Moreover, \hat{f}_c^i only has components of $\hat{f}_{c1[2]}^i$ and $\hat{f}_{c2[2]}^i$ due to the mentioned immobility and the constraints.

$$\theta_h = 0 : [y_1; y_2; f_{c1[2]}^i; f_{c2[2]}^i; \tau_{c1[3]}^{b1}; \tau_{c3[3]}^{b3}] \in \mathbb{R}^6$$

We summarize the simulation results of the NODA model by supervised learning for 20 epochs with the Adam optimizer in Table I. 130k sample and label data are collected by Algorithm 2. This result shows that the solutions in the previous section successfully capture the features of the infinite number of optimal solutions to the non-convex problem.

REFERENCES

- [1] Qiji Ze, Shuai Wu, Jun Nishikawa, Jize Dai, Yue Sun, Sophie Leanza, Cole Zemelka, Larissa S. Novelino, Glaucio H. Paulino, Ruike Renee Zhao, "Soft robotic origami crawler," *Science Advances*, 8(13), p.eabm7834.
- [2] N. Bellini, "Magnetic Actuators for Nanosatellite Attitude Control," PhD thesis, Universita' di Bologna, 2014.
- [3] Abbott, J.J., Brink, J.B. and Osting, B., 2017. Computing minimum-power dipole solutions for interdipole forces using nonlinear constrained optimization with application to electromagnetic formation flight. *IEEE Robotics and automation letters*, 2(2), pp.1008-1014.

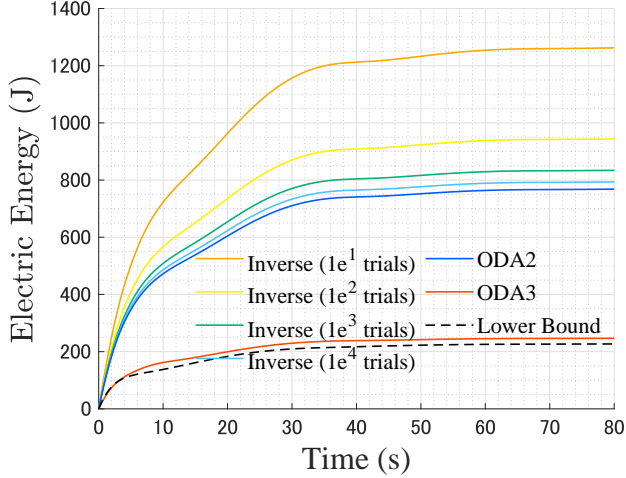


Fig. 6: Simulation results of energy consumptions for each dipole allocation method.

TABLE I: Hyperparameters for Neural Optimal-power Dipole Allocation” (NODA).

Allocations	Pseudo-Inv. $\times 1e^4$	IR ₂ $\times 1e^4$	ODA ₂	ODA ₃	NODA ₃
Command	$u_c = B_{(3,2)}^{-1} M_{(3,2)} S_{(3,2)} u_x$				
Grouping	Decentralized			Centralized	
Ave. [%]	0.092	-	0.095	0.69	0.99
Intef [%]	2.4	6.9	2.6	0.46	0.22
Maxf [%]	5.4	-	5.15	0.40	0.36
Ave. [%]	0.092	-	0.095	0.69	0.6
Inte τ [%]	0.9	$5.6e^3$	0.6	1.9	0.70
Max τ [%]	5.1	-	5.0	0.53	0.5
Time [s]	$\frac{4.2e^{-1}}{1e^4}$	$\frac{7.4e^{-1}}{1e^4}$	2.5	1.0	$1e^{-2}$
Power [J]	800-1200	-	750	250	220

[4] S.I. Sakai, Y. Fukushima, and H. Saito, “Design and on-orbit evaluation of magnetic attitude control system for the “REIMEI” microsatellite,” *10th IEEE International Workshop on Advanced Motion Control*, pp. 584-589, 2008, March.

[5] Aya, S., “Micro-electromagnetic formation flight of satellite systems,” Master diss., Massachusetts Institute of Technology, 2005.

[6] Ivanov, D., Gondar, R., Monakhova, U., Guerman, A., and Ovchinnikov, M., “Electromagnetic Uncoordinated Control of a ChipSats Swarm Using Magnetorquers,” *Acta Astronautica*, Vol. 192, 2022, pp. 15-29.

[7] Takahashi, Y., Sakamoto, H. and Sakai, S., “Simultaneous Control of Relative Position and Absolute Attitude for Electromagnetic Spacecraft Swarm,” *AIAA Scitech 2021 Forum*, 2021. <https://doi.org/10.2514/6.2021-1104>

[8] Takahashi, Y., Sakamoto, H. and Sakai, S., “Kinematics Control of Electromagnetic Formation Flight Using Angular-Momentum Conservation Constraint,” *Journal of Guidance, Control, and Dynamics*, Vol. 45, No. 2, 2022, pp. 280-295. <https://doi.org/10.2514/1.G005873>

[9] Takahashi, Y., Sakamoto, H. and Sakai, S., “Control Law of Electromagnetic Formation Flight Utilizing Conservation of Angular Momentum: Time-Varying Control without Using Additional Attitude Actuator,” *The 30th Workshop on JAXA Astrodynamics and Flight Mechanics*, 2020.

[10] Tajima, H., Takahashi, Y., Shibata, T., and Sakai, S., “Study on Short Range Formation Flight and Docking Control Using AC Magnetic Field,” *74th International Astronautical Congress, Baku, Azerbaijan*, 2-6 October 2023.

[11] Shim, S., Takahashi, Y., Usami, N., Kubota, M. and Sakai, S., “Feasibility Analysis of Distributed Space Antennas Using Electromagnetic Formation Flight,” *Proceedings of the 2025 IEEE Aerospace Conference*, to be presented, 2025.

[12] Y. Takahashi, S. Shim, and S.-i. Sakai, “Distance-based relative orbital transition for palm-sized satellites with guaranteed escape-avoidance,” in *AIAA Scitech 2025 Forum*. American Institute of Aeronautics and Astronautics, 2025, accepted.

[13] Schweighart, S. A., “Electromagnetic Formation Flight Dipole Solution Planning,” Ph.D. Thesis, Massachusetts Inst. of Technology, 2005.

[14] Hariri, N.G., “Vision-Based Navigation for Electromagnetic Formation Flight,” Diss. Florida Institute of Technology, 2018.

[15] Alvarez, D.A., “Multi-Degree of Freedom Position and Attitude Control of RINGS Dipoles Using Electromagnetic Forces and Torques,” 2021, <https://repository.fit.edu/etd/1014/>.

[16] Porter, A., Alinger, D., Sedwick, R., Merk, J., Opperman, R., Buck, A., Eslinger, G., Fisher, P., Miller, D., and Bou, E., “Demonstration of Electromagnetic Formation Flight and Wireless Power Transfer,” *Journal of Spacecraft and Rockets*, Vol. 51, No. 6, 2014, pp. 1914–1923. <https://doi.org/10.2514/1.A32940>

[17] Sunny, A., “Single-Degree-of-Freedom Experiments Demonstrating Electromagnetic Formation Flying for Small Satellite Swarms using Piecewise Sinusoidal Controls,” Master Theses and Dissertations–Mechanical Engineering, 146, 2019.

[18] Nurge, M. A., Youngquist, R. C., and Starr, S. O., “A Satellite Formation Flying Approach Providing Both Positioning and Tracking,” *Acta Astronautica*, Vol. 122, 2016, pp. 1-9.

[19] Abbasi, Z., Hoagg, J.B. and Seigler, T.M., “Decentralized Electromagnetic Formation Flight Using Alternating Magnetic Field Forces,” *IEEE Transactions on Control Systems Technology*, 2022.

[20] Mesbahi, M., and Egerstedt, M., *Graph Theoretic Methods in Multiagent Networks*, Princeton University Press, 2010. Triangulation,” *Int. J. Comput. Inf. Sci.*, Vol. 9, No. 3, 1980, pp. 219–242.

[21] Roth, W. E., “On Direct Product Matrices,” *Bulletin of the American Mathematical Society*, Vol. 40, 1934, pp. 461–468.

[22] Boyd, S. P., and Vandenberghe, L., *Convex Optimization*, Cambridge university press, 2004, p229.